Enhancement of the Antifungal Properties of Zataria Multiflora Essential Oil Thorough Combination With Zno Nanomaterial

Samira Enayati
University of Mohaghegh Ardabili
Mahdi Davari (mdavari@uma.ac.ir)
University of Mohaghegh Ardabili
Aziz Habibi-Yangjeh
University of Mohaghegh Ardabili
Asgar Ebadollahi
University of Mohaghegh Ardabili
Solmaz Feizpoor
University of Mohaghegh Ardabili

Research Article

Keywords: Antifungal activity, Essential oil, Fusarium, Green Synthesis, Zataria multiflora, ZnO

Posted Date: March 9th, 2021

DOI: https://doi.org/10.21203/rs.3.rs-276102/v1

Abstract

Fusarium is one of the most important and destructive phytopathogenic fungi on a wide range of host plants. In the present study, to achieve a suitable alternative for high-risk synthetic chemicals, the antifungal effects of ZnO and ZnO-EO (*Zataria multiflora* Boiss essential oil loaded on ZnO) materials were investigated against six isolates of *Fusarium*. The chemical composition of *Z. multiflora* essential oil (EO) was explored by GC-MS, in which thymol and carvacrol were the main components. The physio-chemical properties of fabricated materials were studied by SEM, BET, FT-IR, TGA, EDX, XRD, and DLS analyses. The mycelial growth inhibitory (MGI) of ZnO and ZnO-EO materials were tested against *Fusarium oxysporum* f.sp. *lycopersici*, *F. oxysporum* f.sp. *lentis*, *F. graminearum*, *F. graminearum*, *F. verticillioides*, and *F. brasilicum* in the laboratory conditions. The results showed that ZnO-EO nanocomposite had a fungistatic effect against all tested fungi except *F. oxysporum* f.sp. *lentis* and the fungicidal activity against *F. graminearum* at a concentration of 1000 ppm. The MGI of ZnO-EO nanocomposite was increased by 42.70% compared to the pure ZnO and by 66.33% compared to *Z. multiflora* EO. The MGI of pure ZnO compared to *Z. multiflora* EO was also increased by 23.63%. According to the current findings, the ZnO-EO nanocomposite can be considered as a bio-rational efficient alternative to conventional chemical fungicides.

1. Introduction

One of the most destructive agents in agriculture is phytopathogenic fungi. A significant portion of plant products is annually lost due to plant diseases, while more than 800 million people suffer from food deficiency worldwide (1Strange and Scott 2006). Although most fungal species are saprophyte, plants are attacked by about 270,000 fungal species (2De Lucca 2007). Pathogenic fungi alone cause to reduce main food products by 20 percent throughout the world (3Fisher et al. 2012; 4Gauthier 2013; 5Jampilek 2016; 6Deepak and Yogeshvari 2019). Concerns about the negative effects of synthetic chemicals such as human health threat, environmental pollution, low effectiveness in the management of soil-borne diseases, and the emergence of resistant variety have encouraged researchers to find suitable alternatives (7Davari and Ezazi 2017). The use of eco-friendly agents such as plant essential oils and nanomaterials to the management of plant diseases has been strongly raised in the recent decades (8Adetunji et al. 2017).

Plant essential oils contain a wide range of secondary metabolites, which have antimicrobial, allopathic, antioxidant, and bioregulation properties. Chemically, essential oils are complex compounds containing a variety of chemicals, including hydrocarbons, alcohols, ketones, aldehydes and so on (9Plotto et al. 2003; 10Leimann et al. 2009). Researches have shown that essential oils have many benefits over industrialized fungicides. They have effective compounds that fungi cannot deactivate them. Lack of negative side-effects, rapid decomposition, and the impact on a wide range of pathogens are among the other benefits of essential oils (11Shavisi et al. 2017).

Despite desirable antifungal and antimicrobial properties, the essential oils of aromatic plants have limitations in their instability and degradation against environmental factors such as light, oxygen, moisture, and pH (12Donsi et al. 2011). One of the applicable ways to solve the problems associated with the volatility and instability of essential oils is nano-encapsulation (13Ojha et al. 2018; 14Kedia et al. 2018). Nanomaterials, in general, can cause slow release and effective delivery in disease management (15Duhan et al. 2017). Also, nanometric size delivery systems, due to the subcellular size, may enhance the passive cellular absorption mechanisms, consequently diminishing mass transfer resistances and improving antimicrobial and antifungal activity (12Donsi et al. 2011). Moreover, solid nanomaterials protect essential oils against environmental factors such as oxygen, moisture, light, and acidity, also create nano-sized carriers, easily increase the solubility and bioavailability of essential oils, and improve their controlled release (16Raut and Karuppayil 2014; 17Elmer and White 2018). Various researches have evaluated the antifungal effects of essential oils and nanomaterials. For example, the antifungal activity of Fe_3O_4/ZnO/AgBr, TiO_2-RGO, and SiO_2/Ag_2S composites has been investigated against several phytopathogenic fungi including *Fusarium graminearum, F. solani*, *F. oxysporum*, and *Aspergillus niger* (18Sara et al. 2009; 19Fernandez et al. 2014; 20Hoseinzadeh et al. 2016). Nanoparticles of zinc oxide (ZnO NPs) has been also applied in various antifungal investigations, which showed that these NPs possess significant potential to diminish the growth of phytopathogenic fungi (21 Kalia et al. 2020). A study on the antifungal activity of CuO/ZnO nanocomposites by 22Kankanit et al. (2013) also showed that these nanocomposites had inhibitory properties on the growth of *Trichoderma* spp. 23kim et al (2012) also reported the significant antifungal effects of silver nanoparticles on eighteen fungi pathogenic on fruits and cereals.

To the best of our knowledge, there is not any research about the inhibitory of *Zataria multiflora* essential oil integrated with ZnO nanomaterials on the mycelial growth of pathogenic fungi. Herein, we combined ZnO with *Z. multiflora* essential oil using one-pot ultrasonic-assisted method, and the antifungal performance of ZnO and ZnO-EO (*Zataria multiflora* Boiss essential oil loaded on ZnO) materials were investigated against six isolates of *Fusarium* and the results were discussed.

2. Materials And Methods

2.1. Preparation of pathogenic fungi

In this study, six important pathogenic strains of *Fusarium* genus, including *Fusarium oxysporum* f.sp. *lycopersici* UM0.004 (causal agent of tomato wilting), *F. oxysporum* f.sp. lentis FL6 (causal agent of lentil wilting), *F. graminearum* UM89 (CBS131571), *F. graminearum* UM29 (CBS389.62) (causal agent of wheat head blight), *F. verticillioides* (CBS 218.76) (causal agent of corn cob rot), and *F. brasilicum* (CBS119179) (causal agent of barley head blight) were used. The fungi were identified by morphological and molecular methods and were received from CBS-KNAW culture collection or Fungal Collection of University of Mohaghegh Ardabili (FCUMA).

2.2. Preparation and analysis of essential oil

Zataria multiflora essential oils were provided from Barij Essential oil Company (Kashan, Iran). The essential oil was analyzed by a Gas Chromatography (HP-7890B) coupled with a Mass Spectrometer (Agilent-MSD5975C). The length, diameter, and film thickness of HP-5MS column were 30 m, 025 mm, and 0.25 µm, respectively. Helium (99.99%) was used as carrier gas with a flow rate of 1 mL per minute. Identification of each component was made by comparing its retention time and mass spectra fragmentation with those stored in the computer libraries; Wiley 7n 0.1 (Wiley, NY) and NIST (Standard Reference Data, Gaithersburg).

2.3. Antifungal effect of *multiflora* essential oil in laboratory conditions

The antifungal effect of EO on six pathogenic strains of *Fusarium* was performed by mixing different concentrations of EO with PDA medium. Briefly, the emulsion of the essential oil was prepared with 0.05% (v/v) Tween 80 and blended with sterile PDA at 40-45 ºC to obtain a final concentration of 600 µl/L of *Z. multiflora* EO. Then, this medium was divided into 9 cm Petri dishes and allowed to coagulate. A 5 mm mycelial disc from young cultures of target fungi was placed in treated plates. In control plates, only Tween 80 was used. Inoculated plates were sealed with parafilm in order to prevent exhaust of the essential oil, and placed in an incubator at 25 ºC. The experiment was performed in three repeats. After 48 hours, the vegetative growth of fungal colonies was measured daily until the surface of the culture medium of control petri dishes was completely occupied by the fungus. The inhibitory percentage of different concentrations of essential oil was determined using Abbott's formula: IP = (C-T / C) × 100, in which IP = inhibitory percentage, C = the mean diameter of the fungus colony in the control treatment, and T = the mean diameter of the fungus colony in the mentioned treatment (7Davari and Ezazi, 2017).

2.4. Synthesis of ZnO

For this purpose, 3.65 g Zn $(NO_3)_2.6H_2O$ (Loba chemie, India) was added to 100 mL of water. The solution was placed on a mixer (Heidolph model, Germany) at 450 rpm for 30 minutes at 25 °C and its pH was adjusted to 10 using NaOH. The prepared solution was then placed in an ultrasonic device (Bandelin model HD 3100) with water circulation within 2 hours. Thereafter, the prepared ZnO was separated by centrifuge and dried in an oven within 24 hours (24Pirhashemi and Habibi-Yangjeh 2017).

2.5. Combination of *multiflora* essential oil with ZnO

To synthesize ZnO-EO (ZnO/essential oil of *Z. multiflora*), 3 g Zn $(NO_3).6H_2O$ was added to 90 mL water. Then, 1 mL of *Z. multiflora* EO was dissolved in 9 mL of ethanol and added to the above solution. The pH of the solution was adjusted to 10 and placed for half an hour on a mixer at 450 rpm. Then, it was ultrasonicated for 2 hours and separated and dried similar to the ZnO sample.

2.6. Characterization of the materials

XRD patterns were performed using Cu-K radiation. Surface morphology was assessed using SEM (LEO 1430VP model, Germany) with 15 kV accelerator voltage. A FT-IR was used to examine the vibrational

spectra of the samples. For this purpose, a mixture of the material with KBr powder was prepared in 1 to 10 ratio and the position of their peaks was examined in the frequency range from 400 to 4000 cm^{-1}. Material purity and analysis of elements in the synthesized products were investigated by EDX (Rontec GmbH, Germany). Thermo-gravimetric *analysis* was used to investigate the differences in thermal stability of samples in the temperature range from 31 to 700 °C with TGA/DTA thermal analysis device under air atmosphere. The BET instrument (BELSORP mini model, Japan) was used to investigate the degree of porosity, and the DLS (Dynamic light scattering; HORIBA model, Japan) was used to estimate the size of the particles.

2.7. Antifungal activity of materials

The desired concentrations of ZnO and ZnO-EO materials were prepared and added to PDA in Petri dishes. A 5 mm mycelial disc from young cultures of target fungi was placed in treated plates. At certain time intervals, the mycelial diameters of pathogenic fungi were measured. In this study, the antifungal effects of ZnO and ZnO-EO materials on *Fusarium* isolates were measured by mixing method with PDA (micro-dilution) at concentrations of 75, 150, 300, 600, and 1000 (along with 2000 ppm for ZnO) in a completely randomized design (CRD) in three replications. Mycelial inhibition percentages for each pathogenic fungi were compared with Tukey's text at p = 0.05.

3. Results And Discussion

The analysis of *Z. multiflora* EO represented that thymol (36.18%), carvacrol (32.53%), p-cymene (7.52%), and -Terpinene (5.28%) were the main compounds (Table 1). The results obtained from comparing the mean inhibitory percentages at 2000 ppm showed that ZnO had the greatest mycelial growth inhibitory on the *F. graminearum* UM89 (81.43%), while the lowest growth inhibitory was found on *F. brasilicum* (58.19%) (Fig. 1a). Based on the values of IP_{50}, no significant difference was observed between the studied fungi, and the pure ZnO had the highest and lowest antifungal activity on the growth of *F. graminearum* UM89 and *F. oxysporum* f.sp. *lycopercisi*, respectively. At a concentration of 1000 ppm, 100% growth inhibitory was observed on all pathogenic fungi except *F. oxysporum* f.sp. *lentis* (Fig. 1b and 3b). In order to determine whether ZnO-EO had fungistatic or fungicidal effects, mycelial discs, which did not grow at 1000 ppm were placed on a PDA without inhibition material and examined after one week. The results showed that it has fungistatic property on the mycelial growth of all fungi except *F. graminearum* UM89. In fact, the ZnO-EO nanocomposite had a fungicidal effect on *F. graminearum* UM89. According to probit analysis, there was no significant difference between the tested fungi in terms of the effectiveness of ZnO-EO nanocomposite. Also, this composite had the highest and lowest antifungal activity on the mycelial growth of *F. graminearum* UM89 and *F. oxysporum* f.sp. *lycopercisi*, respectively. The comparison of mean inhibitory percentages in mycelial growth of pathogenic fungi is shown in Fig. 2a. As can be observed, the ZnO-EO nanocomposite has the greatest impact on the growth of the studied fungi. Pure *Z. multiflora* EO at 600 µl/L was compared to the ZnO and ZnO-EO samples on the growth of pathogenic fungi. So that by using a very small amount of essential oil, we are able to significantly increase the effect of ZnO NP. In the ZnO-EO, the mycelial growth inhibitory was increased to

42.70% compared to the ZnO. Inhibitory in the ZnO-EO, compared to pure *Z. multiflora* EO, has also been increased to 66.33%. Mycelial growth inhibitory in ZnO was 23.26% higher than pure *Z. multiflora* EO (Fig. 2b and 3a).

The use of essential oils in the control of plant diseases has been proposed as an effective and safe method in recent years (25Raveau et al. 2020). However, the application of EOs can be associated with some limitations such as high cost, evaporation in high temperature, instability in high pressure, and decomposition with oxygen (26Joel et al. 2019). Therefore, in the present study, enhancing the efficiency of *Z. multiflora* EO was investigated by combination with ZnO (27Patra and Goswami 2012). The main constituents of *Z. multiflora* EO were thymol and carvacrol. In the previous studies, thymol and carvacrol were also reported as the main constituents of this essential oil (28Mahboubi et al. 2017). Both compounds are phenolic monoterpenoids, which represent strong antimicrobial activity (29Naeini et al. 2010). In fact, such terpenes are the main factors in creating the antimicrobial property of essential oils, which penetrate into the cell membrane and cause the cell contents to clot (30Kordali et al. 2008). In the present study, the inhibitory effect of ZnO was investigated on mycelial growth of six pathogenic strains of *Fusarium*. The results showed that increasing the concentration from 1000 ppm did not have a significant effect on the inhibitory rate of mycelial growth of fungi and the optimal amount for ZnO was 600 and 1000 ppm. In previous researches, 31He et al. (2011) reported that high-concentration of ZnO nanoparticles had an inhibitory effect on *Penicillium expansum* and *Botrytis cinerea*. In another study, 27Patra and Goswami (2012) showed that the action mechanism of ZnO derived from Zn $(NO_3)_2$ on the *Aspergillus fumigatus* causes to create cell wall abnormality by hydroxyl and intermediate superoxide radicals, eventually due to high energy transfer in the fungus lead to cell death. 32Mosquera-SanchezIn (2020) showed that the different concentrations of ZnO-NPs significantly inhibited, between 93 and 96%, the growth of *Colletotrichum* sp., while the fungicide showed only an 88% inhibition.

3.1. Characterization of the materials

XRD patterns were taken to specify the crystal phases of the samples, and the patterns are presented in Fig 4. For the ZnO sample, the diffraction peaks are belonging to (100), (002), (101), (102), (110), (103), (200), (112), (201), and (004) crystal planes, which proved the wurtzite structure (JCPDS No. 36-3411) (33Foghahazade et al. 2020). As seen in the obtained XRD patterns, the ZnO-EO sample shows the same XRD pattern of the ZnO sample, confirming that the addition of *Zataria multiflora* Boiss essential oil on the surface of ZnO did not influence on the crystal structure of ZnO. Based on the Debye-Scherrer equation, the crystallite sizes for the ZnO and ZnO-EO were estimated to be 22 and 17 nm. The particle size reduction in the binary sample could be due to the capping feature of the metabolites presented in the *Zataria multiflora* Boiss essential oil, which prevented the crystalline growth of the ZnO. The absence of additional peaks indicates the high purity of the as-obtained samples.

EDS analysis was applied to investigate the elemental composition of the samples and the results are displayed in Fig. 5a. The elements of Zn and O were identified on the surface of ZnO sample. Additionally, the elements of Zn, C, and O were represented in the EDS spectrum of the ZnO-EO sample. The results of

EDS technique demonstrated that the *Zataria multiflora* Boiss essential oil have successfully adhered to the surface of ZnO. For detecting the microstructure of the ZnO and ZnO-EO samples, the SEM technique was applied. As observed in the SEM images (Fig. 5b), the ZnO sample illustrates the spindle-shaped structure. After integrating *Zataria multiflora* Boiss essential oil with ZnO, the morphology of ZnO was markedly changed. So that the binary sample almost presented the spherical-like structure (Fig. 5c).

FT-IR spectroscopy was conducted to explore the chemical bonds of ZnO and ZnO-EO samples. From Fig. 6, the bands at 530 cm^{-1} and 3200-3600 cm^{-1} are related to the stretching vibrations of the Zn-O and O-H groups (34Geetha et al. 2016; 35Srivastava et al. 2013). For the ZnO-EO sample, the absorption peaks appeared at 855 and 1380 cm^{-1} are assigned to the stretching vibration of the C-H and C=C groups, respectively (36Wang et al. 2014; 37Nuri et al. 2019; 38Hsu 1997). It is worth pointing out that the expected peaks have appeared in the FT-IR spectra of the samples, which indicated that the *Zataria multiflora* Boiss essential oil particles are successfully linked to the ZnO surface.

The porous nature and surface area of the samples were studied by BET analysis. Table 2 and Fig. 7 present the information on porosity and N_2 sorption curves of the ZnO and ZnO-EO samples. The isotherms of the samples are classed as isotherm of type II. The surface areas of ZnO is 11.5 $m^2\ g^{-1}$ with pore volumes and mean pore diameters of 0.161 $cm^3\ g^{-1}$ and 56.1 nm, which are higher than those of ZnO-EO sample (3.50 $m^2\ g^{-1}$ with pore volumes and mean pore diameters of 0.1515 $cm^3\ g^{-1}$ and 7.6 nm). The reduction in S_{BET} for ZnO-EO sample can be related to the occupation of the ZnO surface by the deposited *Zataria multiflora* Boiss essential oil molecules.

Dynamic light scattering (DLS) is an effective analysis to examine the particle size distribution of the samples. The DLS results of the ZnO and ZnO-EO samples are demonstrated in Fig. 8. The average particle sizes reduced from 118 nm for ZnO to 93 nm for ZnO-EO. The results of DLS analysis of synthesized ZnO sample displayed that the mean size of ZnO is larger than the ZnO-EO. The smallest size is related to ZnO-EO, which has the greatest effect on growth inhibitory on mycelial growth of fungi. Therefore, particles size can affect the inhibitory value of mycelial growth of fungi.

TG analysis could supply information about the thermal stability of the ZnO and ZnO-EO samples (Fig. 9). The ZnO represents weight loss of 2.5% after heating to 600 °C, due to removal of adsorbed water. In the TGA diagram of ZnO-EO, the weight loss is observed in two parts. The first one is very small and up to about 100 °C. The main reason for this weight loss is the evaporation of water molecules, as seen in the ZnO. The second weight loss is about 17.5%, which occurred at higher temperatures and is assigned to the destruction of organic molecules linked to the surface of ZnO. Therefore, it can be concluded that the active compounds and metabolites of *Z. multiflora* EO combined with ZnO-EO is nearly 15%.

4. Conclusion

The present study was aimed to combine the essential oils from *Z. multiflora* EO to the surface of ZnO and the antifungal activities were investigated against six isolates of *Fusarium*. For this aim, the ZnO-EO

nanocomposite was prepared using a facile ultrasonic-assisted method. The TGA data showed that nearly 15% of the essential oils was combined with the ZnO in the nanocomposite. The XRD, SEM, and DLS analyses displayed that the particle sizes of ZnO-EO nanocomposite is smaller than ZnO, which related to the capping feature of the metabolites presented in the essential oil. The results showed that the antifungal effect of the ZnO after integration with the essential oils from *Z. multiflora* was severely enhanced. Overall, the results lead to consideration of additional research of the potential antifungal activity of the ZnO-EO nanocomposite and ZnO-NPs on phytopathogenic fungi such as *Fusarium* species, an efficient, economical and viable antifungal alternative to be used in plant disease management specially under field conditions.

Declarations

Acknowledgment

The financial support of present work by University of Mohaghegh Ardabili-Iran is acknowledged.

Author contributions

Enayati, S. was performed the experiment, Davari, M. and Habibi-Yangjeh, A. supervised the experiment from the beginning to the end, read and corrected the manuscript and Feizpour, S. and Ebadollahi, A. advised the research, performed nanoparticles synthesis and made statistical analyses.

Conflict of interest

The authors declare that they have no conflict of interests.

References

1. Strange, R. N. & Scott, P. R., Plant disease: A threat to global food security. *Annual Review of Phytopathology* 43: 83–116 (2006)
2. De Lucca, A. J. Harmful fungi in both agriculture and medicine. *Revista Iberoamericana de Micologia* 24: 3–13 (2007)
3. Fisher, M. C. et al. Emerging fungal threats to animal, plant and ecosystem health. *Nature* 484: 186–194 (2012)
4. Gauthier, T. Trypacidin, a spore-borne toxin from *Aspergillus fumigatus*, is cytotoxic to lung cells. *PLoS One* 7: e29906 (2013)
5. Jampilek, J. Design of antimalarial agents based on natural products. *Current Organic Chemistry* 21: 1824. doi: 10.2174/1385272821666161214121512 (2016)
6. Panpatte, D. G. *Nanotechnology for Agriculture: Crop Production & Protection*. Springer Nature Singapore Pte Ltd. 323pp. https://doi.org/10.1007/978-981-32-9374-8 (2019)

7. Davari, M., & Ezazi, R. Chemical composition and antifungal activity of the essential oil of *Zhumeri amajdae*, *Heracleum persicum* and *Eucalyptus* sp. against some important phytopathogenic fungi. *Journal de Mycologie Médicale* 27: 463–468 (2017)
8. Adetunji, C., Oloke, J., Kumar, A., Swaranjit, S. & Akpor, B. Synergetic effect of rhamnolipid from *Pseudomonas aeruginosa* C1501 and phytotoxic metabolite from *Lasiodiplodia pseudotheobromae* C1136 on *Amaranthus hybridus* L. and *Echinochloa crus-galli* weeds. *Environmental Science and Pollution Research* 24(15): 13700–13709 (2017)
9. Plotto, A., Roberts, R. G. & Roberts, D. D. Evaluation of plant essential oils as natural postharvest disease control of tomato (*Lycopersicun esculentum* L.). *Acta Horticulture* 628: 737–745 (2003)
10. Leimann, F. V., Gonçalves, O. H., Machado, R. A., & Bolzan, A. Antimicrobial activity of microencapsulated *lemongrass* essential oil and the effect of experimental parameters on microcapsules size and morphology. *Material Science Engineering* 29(2): 430–436 (2009)
11. Shavisi, N., Khanjari, A., Akhondzadeh Basti, A., Misaghi, A. & Shahbazi, Y. Effect of PLA films containing propolis ethanolic extract, cellulose nanoparticle *and Ziziphora clinopodioides* essential oil on chemical, microbial and sensory properties of minced beef. *Meat science* 124: 95–104 (2017)
12. Donsi, F., Annuanziata, M. Sessa, M. & Ferrari, G. Nano-encapsulation of essential oils to enhance their antimicrobial activity in foods. *Food Science and Technology* 44: 1908–1914 (2011)
13. Ojha, S. et al. *Nanotechnology in Crop Protection.* Chapter 16. Nanomaterials in Plants, Algae, and Microorganisms 1: 345-391 (2018)
14. Kedia, A., & Kishore Dobey, N. Nanoencapsulation of Essential Oils: A Possible Way for an Eco-Friendly Strategy to Control Postharvest Spoilage of Food Commodities from Pests. Nanomaterials in Plants, Algae, and Microorganisms 1: 501–522 (2018)
15. Duhan, J. S. et al. Nanotechnology: the new perspective in precision agriculture. *Biotechnology Reports* 15: 11–23. doi: 10.1016/j.btre.2017.03.002 (2017)
16. Raut, J. S. & Karuppayil, S. M. A status review on the medicinal properties of essential oils. *Industrial Crops and Product* 62: 250–264 (2014)
17. Elmer, W. & White, J.C. The Future of Nanotechnology in Plant Pathology. *Annual Review of Phytopathology* 56: 111–133. doi.org/10.1146/annurev-phyto-080417-050108 (2018)
18. Sara, F., Marcia, C.N., Adelaide, A., Joao, T. & Tito, O. Anti-fungal activity of Sio2/Ag2s nanocomposites against *Aspergillus niger*. Colloids and Surface B: *Biointerface* 74: 304–308 (2009)
19. Fernandez-Ibáñez, P. et al. Solar photocatalytic disinfection of water using titanium dioxide graphene composites. *Chemical Engineering Journal* 261: 36-44 (2014)
20. Hoseinzadeh, A., Habibi-Yangjeh, A. & Davari, M. Antifungal activity of magnetically separable Fe3O4/ZnO/AgBr nanocomposites prepared by microwave-assisted method, Progress in Natural Science: *Materials International* 26: 334–340 (2016)
21. Kalia, A., Abd-Elsalam, K.A. & Kuca, K. Zinc-Based Nanomaterials for Diagnosis and Management of Plant Diseases: Ecological Safety and Future Prospects. *Journal of Fungi*, 6: 222. https://doi.org/10.3390/jof6040222 (2020)

22. Kankanit, P., Mongkol, P. & Pand, W. Study of antifungal activities of Cuo/Zno nanocomposites synthesized by co-precipitation Method. *Advanced material Research* 802: 89–93 (2013)
23. Kim, S.W. et al. Antifungal effects of silver nanoparticeles (AgNPs) against various plant pathogenic fungi. *Mycobiology* 40: 53–58 (2012)
24. Pirhashemi, M. & Habibi-Yangjeh, A. Ultrasonic-assisted preparation of plasmonic ZnO/Ag/Ag2WO4 nanocomposites with high visible-light photocatalytic performance for degradation of organic pollutants. *Journal of Colloid Interface Science*491: 216-229 (2017)
25. Raveau. R., Fontaine, J. & Lounès-Hadj Sahraoui, A. Essential oils as potential alternative biocontrol products against plant pathogens and weeds: A Review. *Foods* 9(3): 365. doi:10.3390/foods90303652020 (2017)
26. Joel, A. et al. Biofungicides as alternative to synthetic fungicide control of grey mould (*Botrytis cinerea*) – prospects and challenges, *Biocontrol Science and Technology* 29: 207-228, doi: 10.1080/09583157.2018.1548574 (2019)
27. Patra, P. & Goswami, A., 2012. Zinc nitrate derived nano ZnO: fungicide for disease management of horticultural crops. *International Journal of Innovations Horticultural* 1: 79–84.
28. Mahboubi, M., Heidarytabar, R. & Mahdizadeh, E. & Hosseini, H. Antimicrobial activity and chemical composition of *Thymus* species and *Zataria multiflora* essential oils. *Agriculture and Natural Resources* 51: 395–401 (2017)
29. Naeini, A. T., Ziglari, H., Shokri, M. & Khosravi, A. R. Assessment of growth inhibiting effect of some plant essential oils on different *Fusarium* isolates. *Journal de Mycologie Médicale* 20: 174–178 (2010)
30. Kordali, S., Ala Gormez, A. & Yildirim, A. Determination of the chemical composition and antioxidant activity of the essential oil of *Artemisia dracunculus* and of the antifungal and antibacterial activities of Turkish *Artemisia absinthium*, *A. dracunculus*, *Artemisia santonicum*, and *Artemisia spicigera* essential oils. *Journal of Agricultural and Food Chemistry* 53: 9452-9458 (2008)
31. He, L., Liu, Y., Mustapha, A. & Lin, M. Antifungal activity of zinc oxide nanoparticles against *Botrytis cinerea* and *Penicillium expansum*. *Microbiological Research* 166 (3): 207–215 (2011)
32. Mosquera-Sánchez, L.P. et al. Antifungal effect of zinc oxide nanoparticles (ZnO-NPs) on *Colletotrichum* sp., causal agent of anthracnose in coffee crops. *Biocatalysis and Agricultural Biotechnology* 25: 101579 (2020)
33. Foghahazade, N. Behnejad, H. Mousavi, M. & Hamzehloo, M. Novel p–n–p heterojunction photocatalyst synthesized by BiFeO3, ZnO, and BiOBr nanoparticles: facile preparation and high photocatalytic activity under visible light. *Journal of Materials Science: Materials in Electronics*31:19764-19777 (2020)
34. Geetha, M., Nagabhushana, H. & Shivananjaiah, H. Green mediated synthesis and characterization of ZnO nanoparticles using *Euphorbia jatropa* latex as reducing agent. *Journal of Molecular Structure* 1(3): 301–310 (2016)

35. Srivastava, V., Gusain, D. & Sharma, Y.C. Synthesis, characterization and application of zinc oxide nanoparticles (n-ZnO). *Ceramics International* 39(8): 9803–8089 (2013)
36. Wang, X., Liu, X., Chen, J., Han, H. & Yuan, Z. Evaluation and mechanism of antifungal effects of carbon nanomaterials in controlling plant fungal pathogen. *Carbon* 68, 798–806 (2014)
37. Nuri, A. et al. Pd supported IRMOF-3: Heterogeneous, efficient and reusable catalyst for heck reaction. *Journal of Polymer Research* 149: 1941–1951 (2019)
38. Hsu, C. P. S. *Infrared spectroscopy.* Handbook of instrumental techniques for analytical chemistry, 249 (1997)

Tables

Table 1. Type and percentage of compounds identified in *Zataria multiflora* essential oil

Percentage of species (%)	Retention time (RT)	Compounds	No.
0.24	5.202	-Thujene	1
3.02	5.333	-Pinene	2
0.21	5.608	Camphene	3
0.31	6.129	-Pinene	4
0.15	6.283	2-Octanone	5
0.57	6.363	Myrcene	6
0.11	6.638	-Fellandrene	7
1.42	6.867	-Terpinen	8
7.52	7.033	p-cymene	9
0.41	7.102	Limonene	10
0.40	7.164	1-Cineole	11
5.28	7.697	-Terpinene	12
1.43	8.543	Linalool	13
0.58	10.592	Terpinene-4-ol	14
0.52	11.044	-terpineol	15
0.71	12.320	Benzene, 2-methoxy-4-methyl(1-methyl)	16
1.16	12.640	Carvacrol methyl ether	17
36.18	14.695	Thymol	18
32.53	15.129	1-Carvacrol	19
1.06	17.006	Thymol acetate	20
1.21	17.676	Carvacryl acetate	21
2.25	19.238	Caryophyllene	22
0.76	19.850	Aromadendrene	23
0.53	21.555	Ledene	24
0.38	23.827	Dehydro-1-isolongifolene	25
0.39	23.976	longifolene	26
99.33			Total

Table 2. Textural properties of the ZnO and ZnO-EO samples.

Total pore volume (cm^3g^{-1})	Mean pore diameter (nm)	Surface area (m^2g^{-1})	Sample
0.1610	56.1	11.5	ZnO
0.0070	7.6	3.8	ZnO-EO

Figures

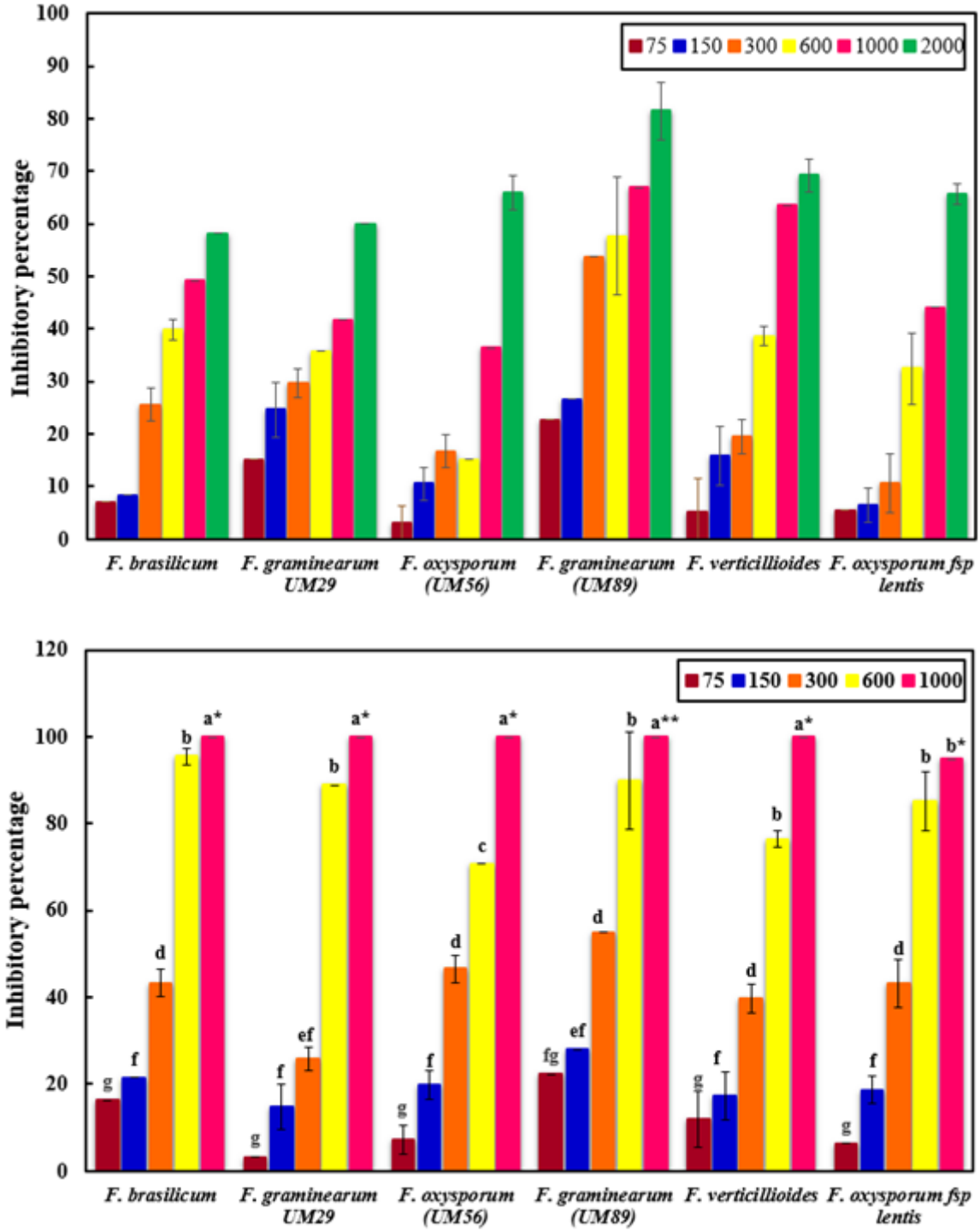

Figure 1

Comparison of the mean inhibitory percentage of mycelial growth of pathogenic fungi with (a) ZnO, (b) ZnO-EO (Z.m). * Indicates the fungistatic property and ** Indicates the fungicidal property.

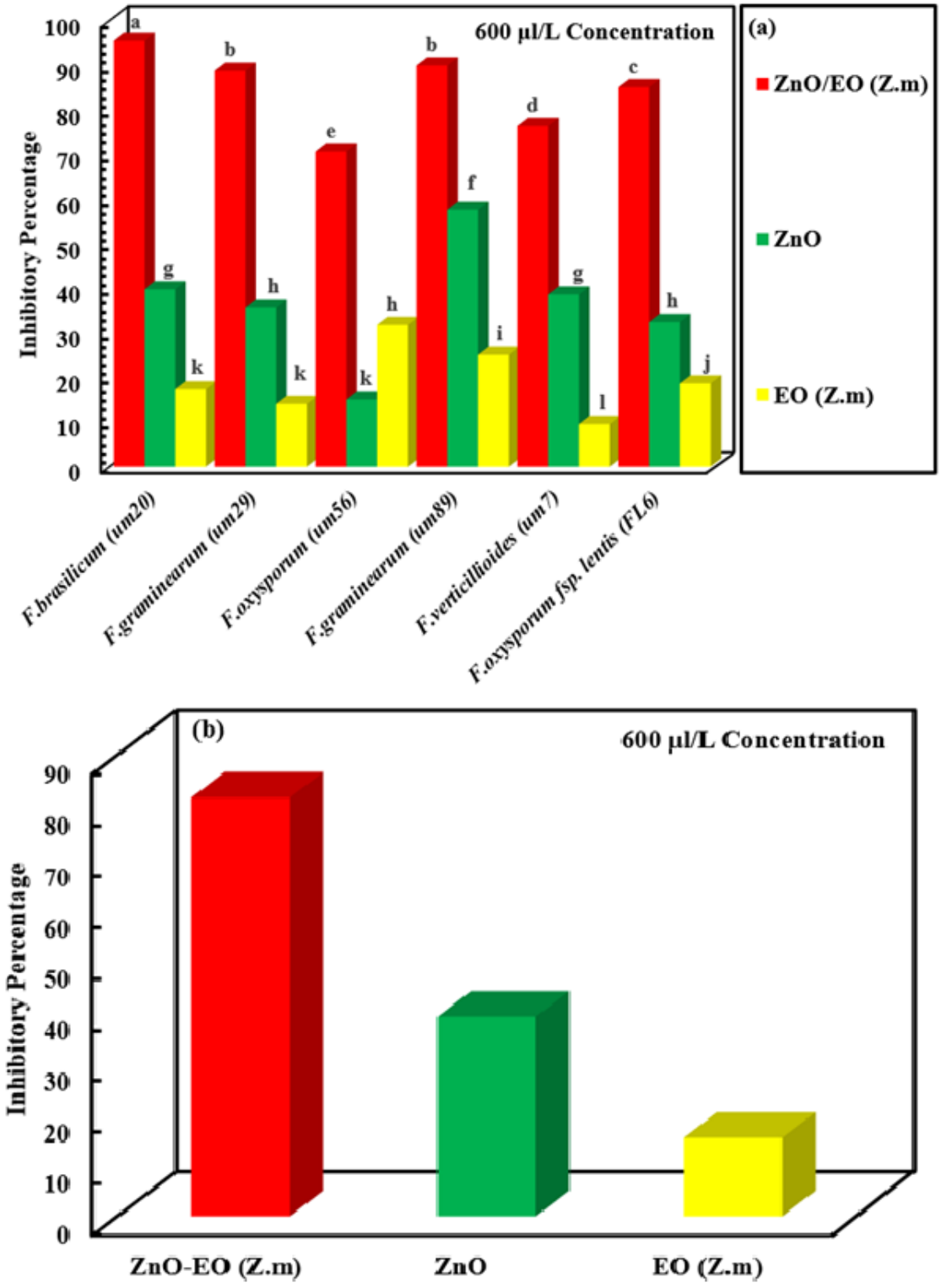

Figure 2

(a) Comparison of the mean inhibitory percentage of ZnO, ZnO-EO and pure Zataria multiflora EO on the mycelial growth of fungi at 600 ppm. (b) Comparison of the inhibitory percentage of all studied fungi at 600 ppm.

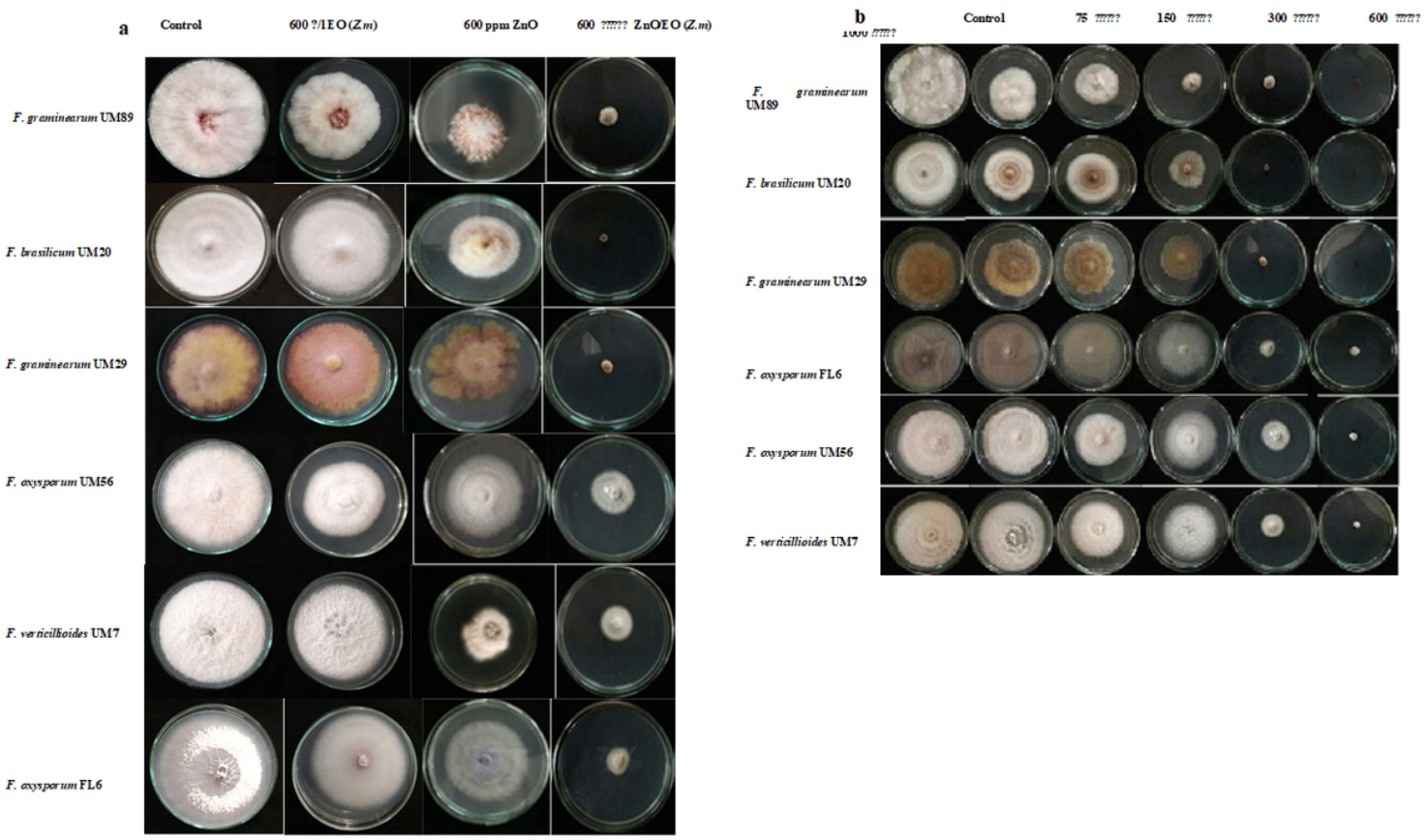

Figure 3

(a) Comparison of Z. multiflora EO, ZnO, and ZnO-EO antifungal activity on the fungi growth at 600 ppm, (b) ZnO-EO antifungal activity on fungal growth at different concentrations.

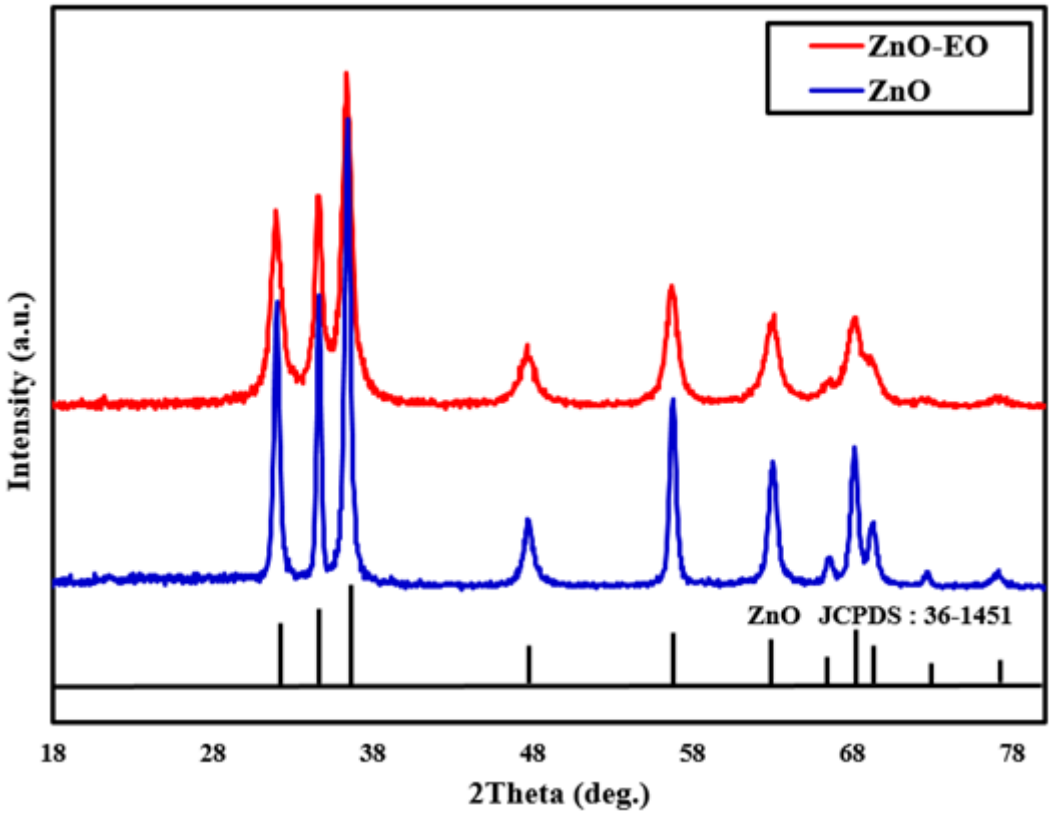

Figure 4

XRD patterns of ZnO and ZnO-EO samples.

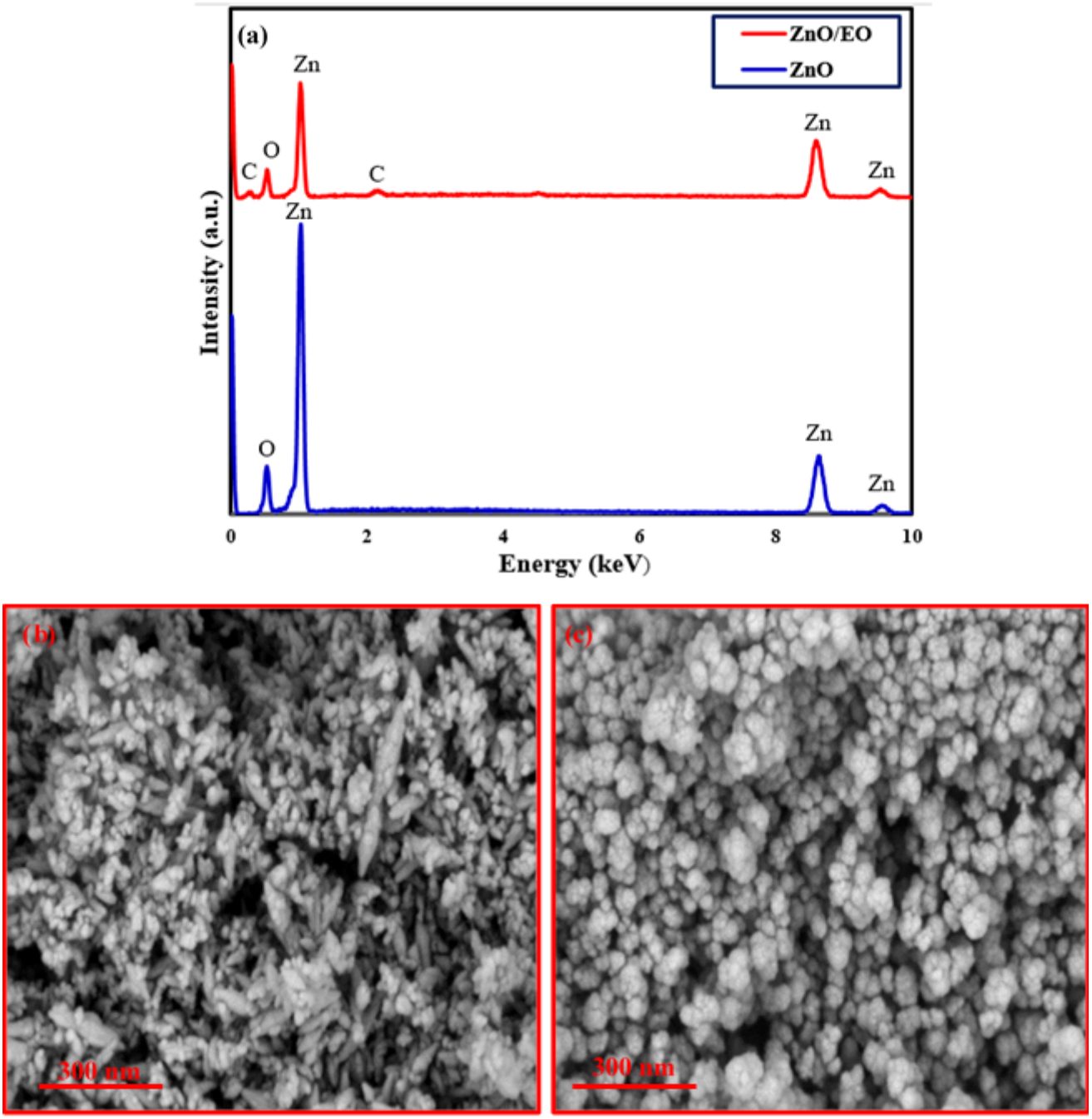

Figure 5

(a) EDS analyses, (b) and (c) SEM images of ZnO and ZnO-EO samples.

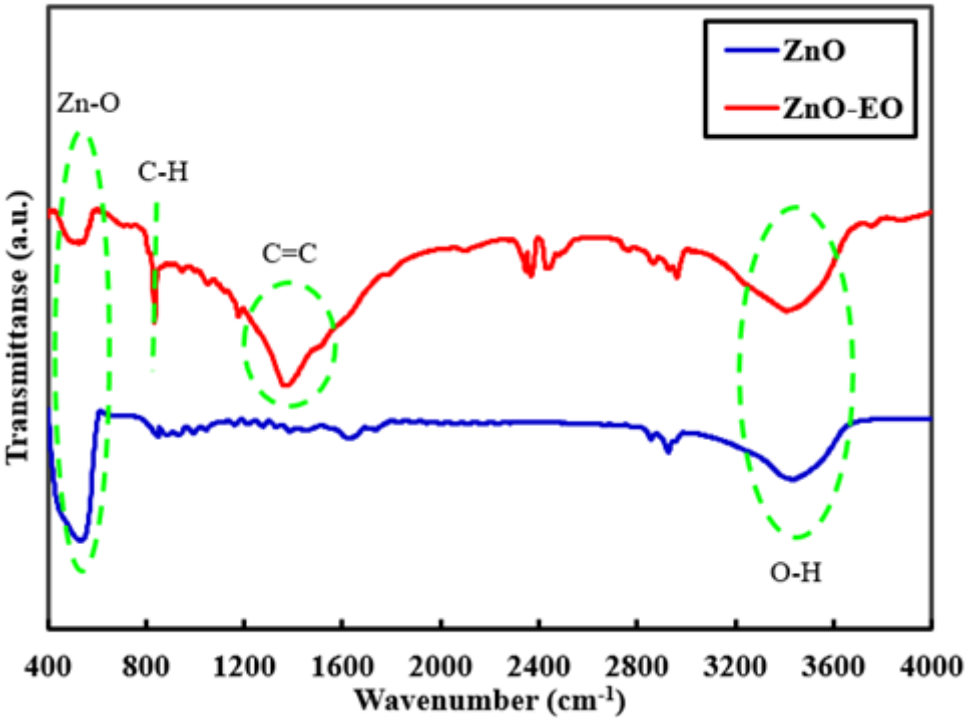

Figure 6

FT-IR spectra of the fabricated samples.

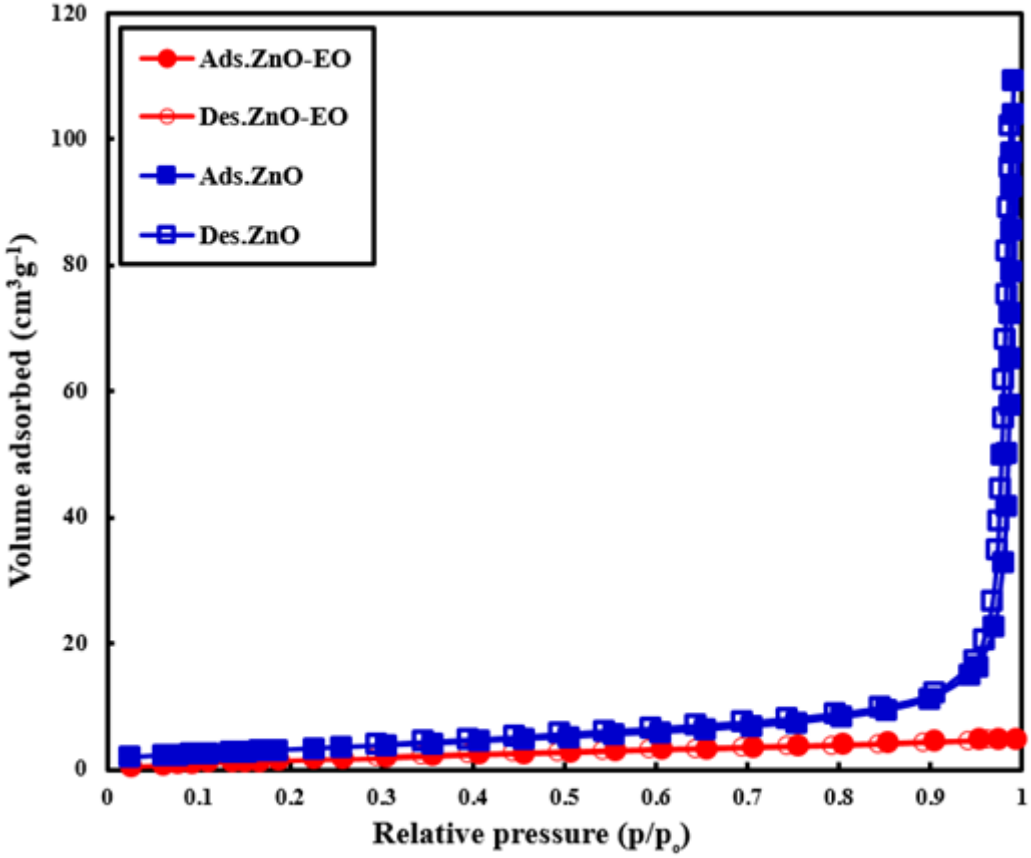

Figure 7

N2 sorption isotherms of the ZnO and ZnO-EO samples.

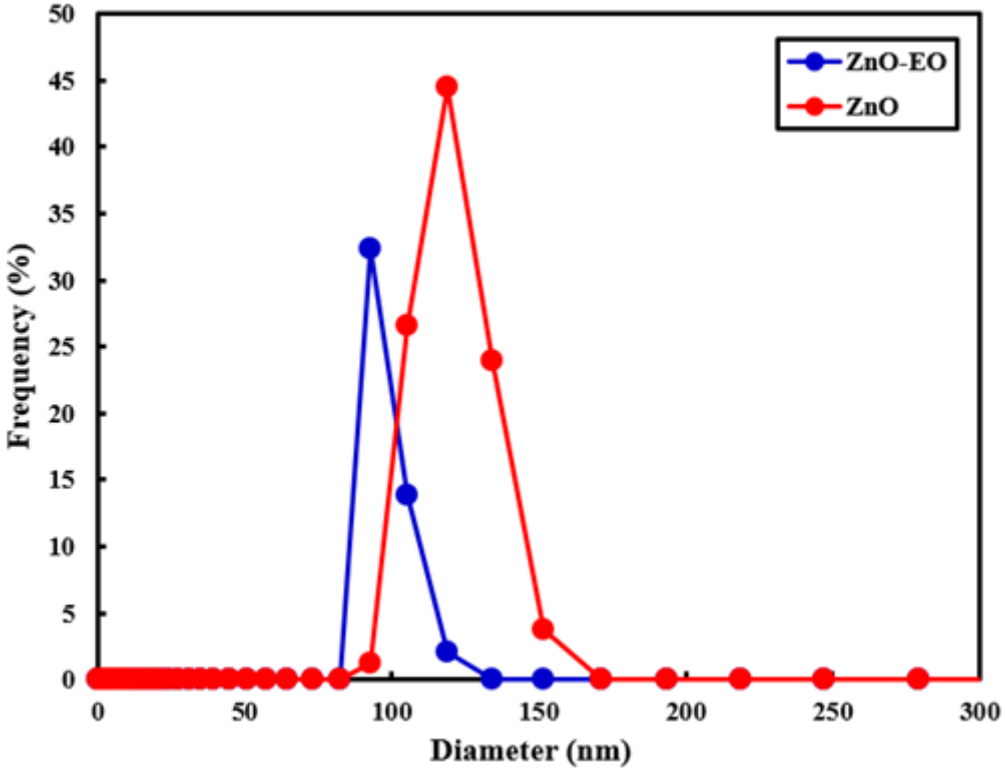

Figure 8

DLS analyses of the ZnO and ZnO-EO samples.

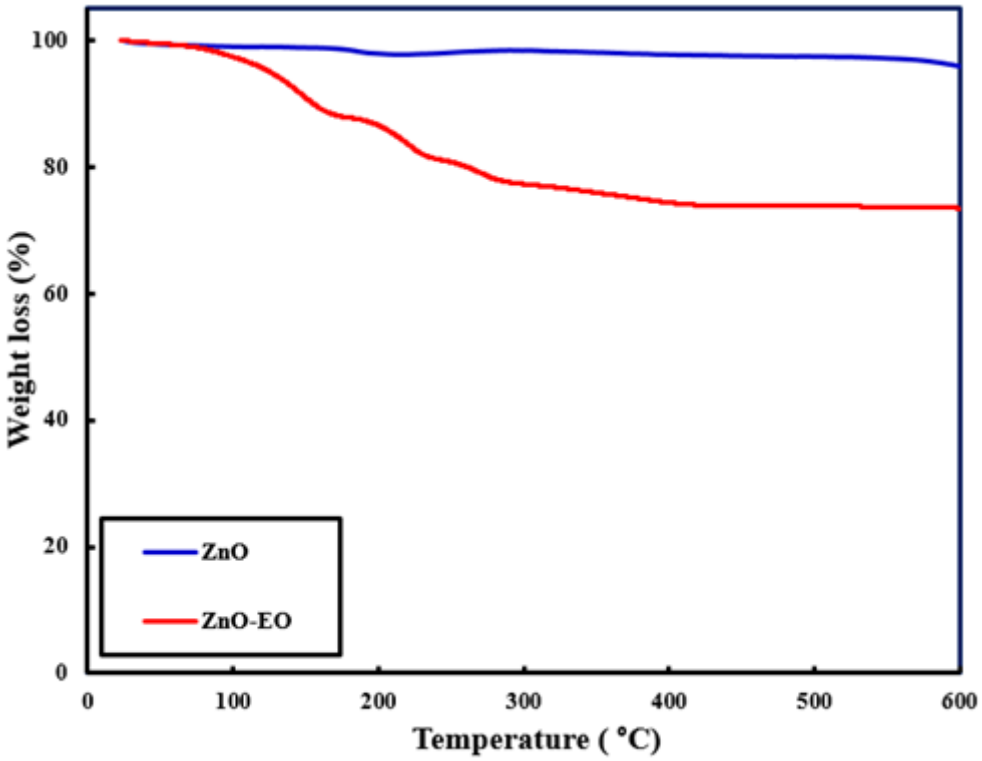

Figure 9

TGA diagrams of the ZnO and ZnO-EO samples.